Supporting Information

Carlyle et al. 10.1073/pnas.1322360111

SI Materials and Methods

For quantitative immunoelectron microscopy, layers II–III of the monkey dorsolateral prefrontal cortex (dlPFC) were sampled for resectioning and analysis under a JEM1010 (Jeol) transmission electron microscope at 80 kV. Immunoreactive structures were digitally captured at 25,000–160,000× magnification (Gatan). For profile identification, we adopted the criteria summarized in ref. 1.

Plastic blocks were examined using the 4th to the 20th surface-most sections (i.e., 160–800 nm; section thickness ≈40 nm), to exclude penetration artifacts. Intense immunolabeling was found to a depth of 2 μm, and was still detectable to a depth of at least 3 μm from the tissue/plastic interface. Data for quantitative assessments were collected from random 46-μm^2 fields of tau phosphorylated at serine 214 (pS214-tau) or phosphodiesterase 4A (PDE4A) immunoperoxidase-labeled material; counterstaining was omitted to facilitate detection.

A total of 1,200 pS214-tau–immunoreactive cellular profiles were counted in young dlPFC neuropil (six tissue blocks from brains 9 y, 10 y, and 11 y; two blocks per brain) and, likewise, 1,200 profiles in aged dlPFC (brains 25 y, 26 y, and 29 y). pS214-Tau profiles were categorized as (*i*) axons, (*ii*) dendritic shafts, (*iii*) dendritic spines, and (*iv*) nondetermined, when safe ultrastructural criteria could not be used for profile identification. The prevalence of PDE4A in dendritic spines was assessed by counting immunoreactive spines within twenty 46-μm^2 fields from five tissue blocks per brain, and counts were normalized to total number of spines in the same area. All eight brains (9–11 y, 24–26 y, 29 y, and 31 y) were used for mapping pS214-tau, PDE4A, and A-kinase anchor protein 6 (AKAP6) with immunoperoxidase or immunogold markers. Vesicular structures exhibiting pS214-tau immunoreactivity were traced in consecutive sections to identify the host cellular profile (i.e., axon, dendritic shaft, or spine) and to capture an association with the plasma membrane or a synaptic junction.

1. Peters A, Palay SL, Webster HdeF (1991) *The Fine Structure of the Nervous System: Neurons and Their Supporting Cells* (Oxford Univ Press, New York).

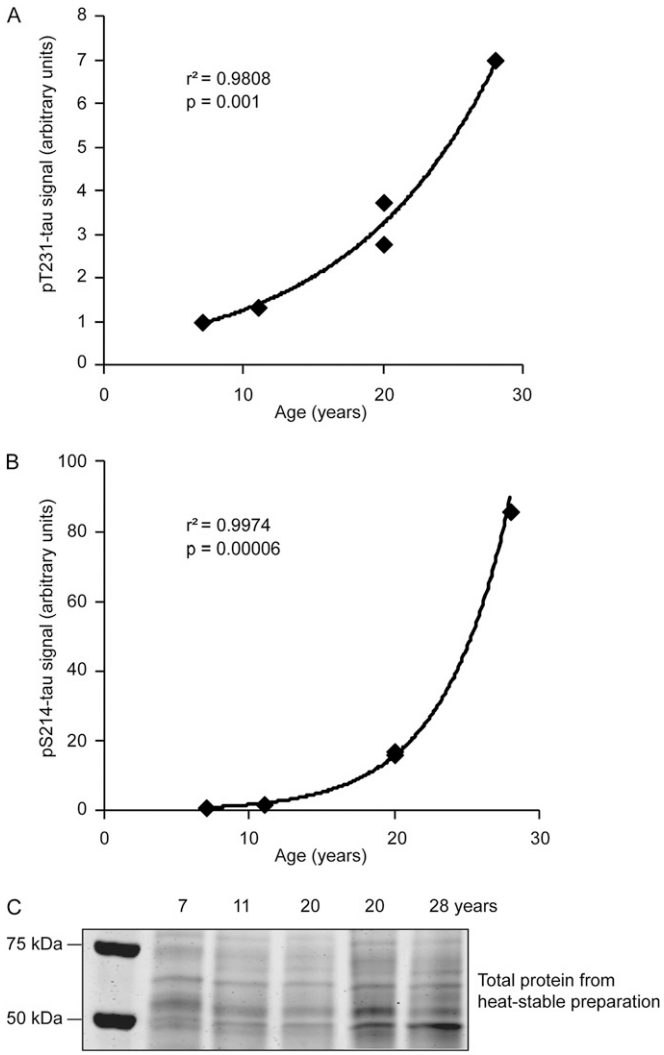

Fig. S1. p-Tau increases in aging monkey dlPFC. (*A* and *B*) Graphs show increasing tau phosphorylation with age at T231 (*A*) and S214 (*B*); fitting to an exponential model shows a highly significant correlation for both phosphorylation sites. Total heat-stable tau band intensity was normalized by total protein from the heat-stable preparation (*C*). Normalized total tau intensity was used to normalize p-tau intensity to produce the graphs. (*C*) To control for total soluble protein in the heat-stable extract, a separate gel was run in parallel and stained with Coomassie blue. The intensity of the whole lane was quantified using Image J, and that number used to normalize total tau band intensity. There was no overall reduction in soluble protein in aged dlPFC, and therefore the decreased levels of soluble tau were not due to a general loss of soluble protein.

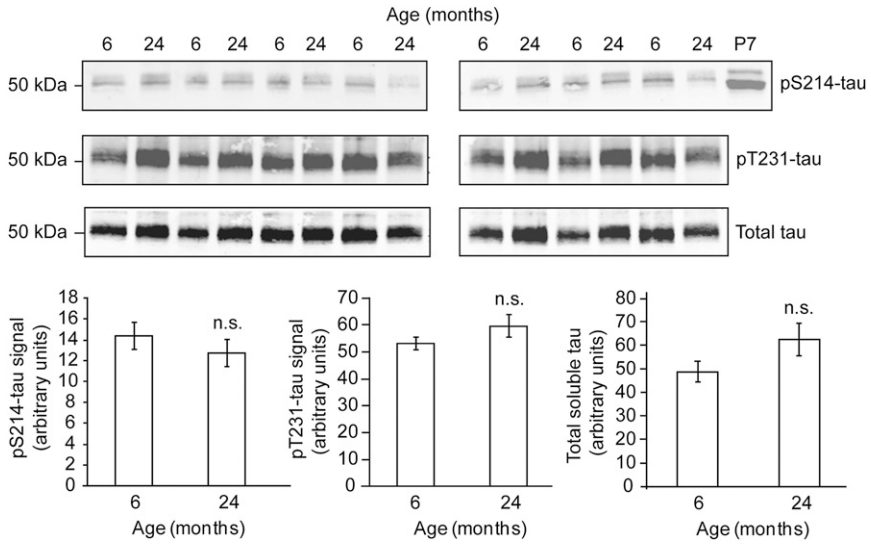

Fig. S2. There is minimal PKA phosphorylation of tau at S214 in adult mouse frontal cortex. Immunoblots of heat-stable protein extracts from whole frontal cortex were labeled for pS214-tau (Millipore; AB9672), pT231-tau (Thermo; PA1-14418), and total tau (Millipore; 05-348, clone 5E2). Quantification showed no significant differences with age for either phosphorylation site or total soluble tau obtained from the preparations. The final lane on the pS214-tau blot shows P7 total mouse brain as a positive control, given low signals in adult mouse brain. Error bars represent SEM.

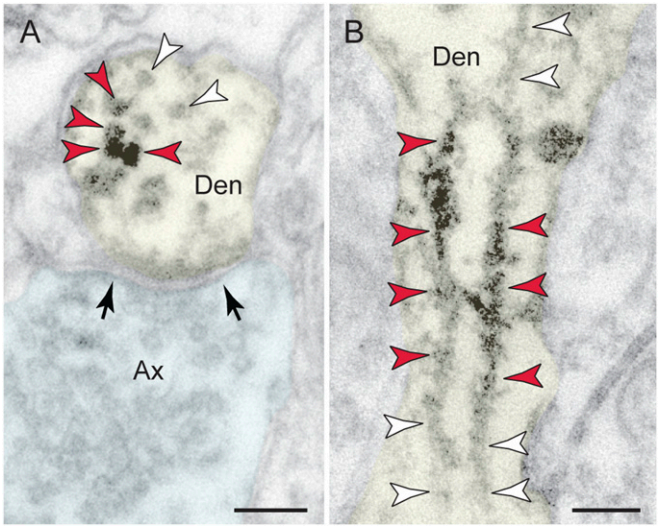

Fig. S3. (*A* and *B*) Subcellular expression of pS214-tau in dendritic shafts of the aged monkey dlPFC. p-Tau aggregates along the microtubules of small caliber, high-order dendrites. *A*, cross section; *B*, longitudinal section. Note that a single microtubule may present intermittent reactivity along its length (red and white arrowheads point to p-tau–reactive and nonreactive microtubules/microtubule sections, respectively). Unlike asymmetric synapses on spines (e.g., Fig. 2*A*), the asymmetric synapse onto the dendrite in *A* (black arrows) is not p-tau immunoreactive. Ax, axon; Den, dendrite. *A* and *B* are pseudocolored for clarity. (Scale bars: 100 nm.)

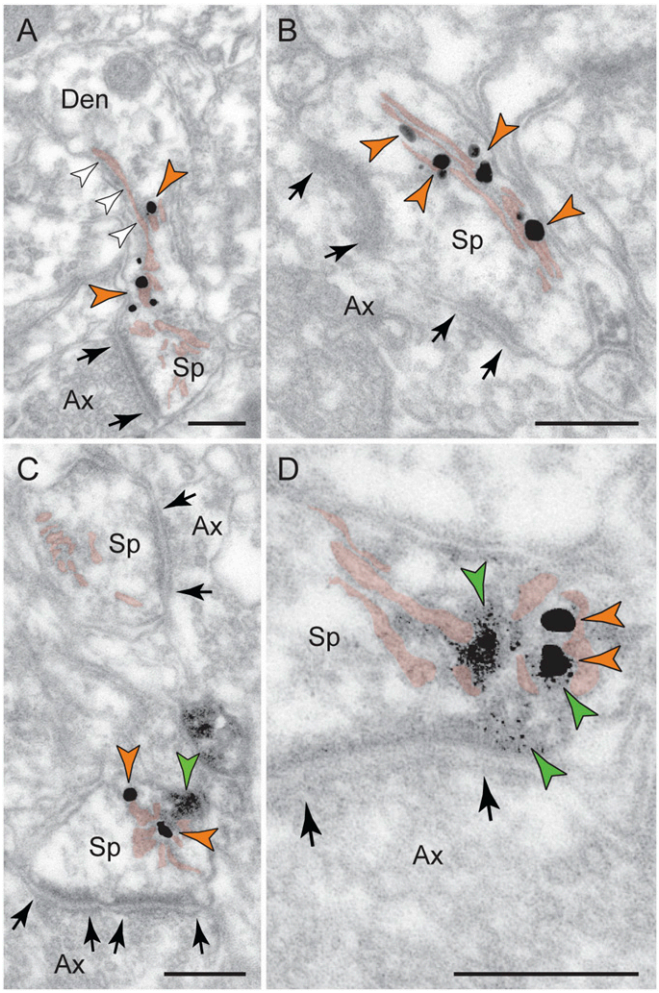

Fig. S4. AKAP6 localization and colocalization with PDE4A in young monkey dlPFC. PKA is tethered by anchoring proteins, including AKAP6. These images document AKAP6 on the spine apparatus (SA) (pseudocolored), the specialized smooth endoplasmic reticulum (SER) that buffers Ca^{2+} in the spine. Internal Ca^{2+} release is mediated via channels on the SA-limiting membrane, namely inositol trisphosphate receptors (IP3Rs) and ryanodine receptors (RYRs); in monkey dlPFC, IP3Rs are localized on SER cisterns, including the SA (1). cAMP-PKA signaling increases internal Ca^{2+} release by increasing the efficacy and expression of IP3Rs (2) and by increasing Ca^{2+} leak through RyRs (3). Increased Ca^{2+} can in turn promote cAMP production, fueling feedforward signaling (2). (*A*–*D*) AKAP6 is selectively localized (orange arrowheads) on the SA, the extension of the dendrite's smooth reticulum into the spine; note in *A* the continuity with the SER of the parent dendrite (white arrowheads). Double immunoEM (*C* and *D*) demonstrates AKAP6 (immunogold, orange arrowheads) colocalization with PDE4A (immunoperoxidase, green arrowheads) on the SA. Thus, PDE4A is positioned to regulate feedforward cAMP-Ca^{2+} signaling in dlPFC spines. Arrows point to asymmetric axospinous synapses. Ax, axon; Den, dendrite; Sp, spine. (Scale bars: 200 nm.)

1. Paspalas CD, Goldman-Rakic PS (2004) Microdomains for dopamine volume neurotransmission in primate prefrontal cortex. *J Neurosci* 24(23):5292–5300.
2. Arnsten AF, Wang MJ, Paspalas CD (2012) Neuromodulation of thought: Flexibilities and vulnerabilities in prefrontal cortical network synapses. *Neuron* 76(1):223–239.
3. Liu X, et al. (2012) Role of leaky neuronal ryanodine receptors in stress-induced cognitive dysfunction. *Cell* 150(5):1055–1067.

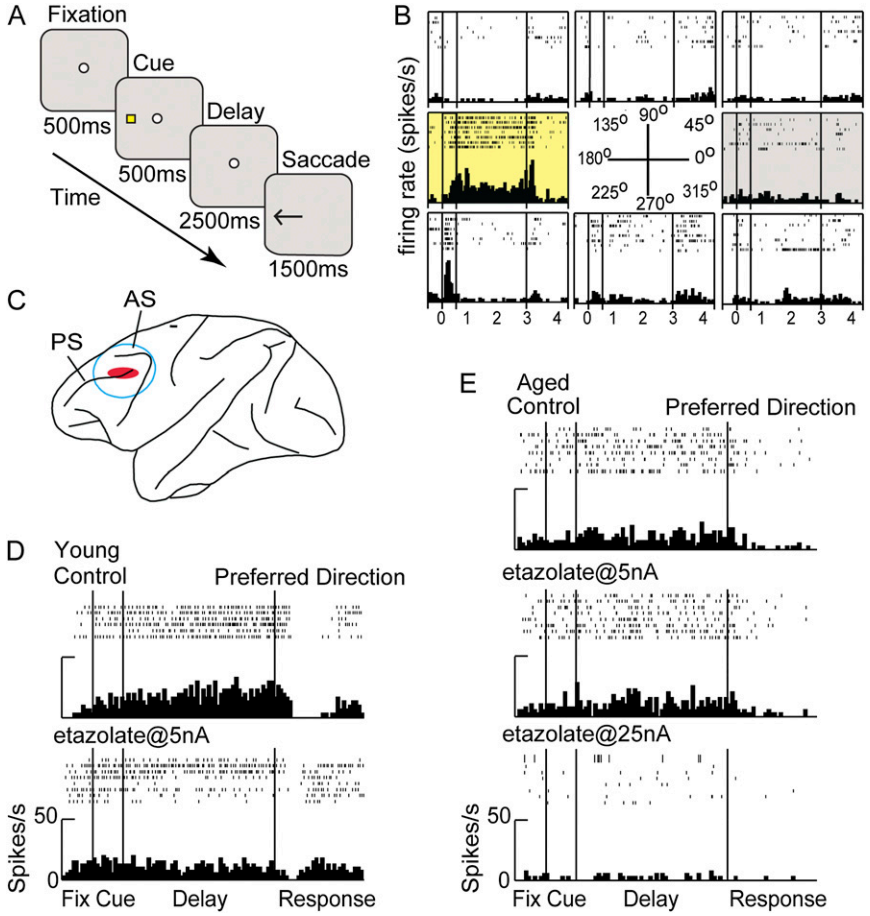

Fig. S5. The PDE4 inhibitor, etazolate, has more potent effects on dlPFC neurons of young than aged monkeys performing a spatial working-memory task. (*A*) The oculomotor delayed response (ODR) task, a test of spatial working memory. The subject begins a trial by fixating at the central spot (fixation period), whereupon a cue is illuminated for 0.5 s (cue period) at one of eight peripheral targets. After the cue, a 2.5-s delay period follows. The subject is required to maintain central fixation throughout both the cue presentation and the delay period. At the end of the delay, the fixation spot is extinguished, instructing the monkey to respond with a memory-guided saccade to the location where the cue had been shown before the delay period. A trial is considered successful if the response is completed within 0.5 s of the offset of the fixation spot and within 2° around the correct cue location; every successful response is rewarded with fruit juice. The stimulus position is randomized over trials (2-s intertrial intervals) such that it has to be remembered on a trial-by-trial basis. (*B*) An example of a dlPFC "delay cell" with spatially tuned persistent firing across the delay period, the neuronal representation of visual space. The yellow highlight indicates the preferred direction of the neuron; gray shading shows the antipreferred direction. (*C*) The dlPFC recording site in the caudal portion of the principal sulcus (PS) near the arcuate sulcus (AS). This is the region that receives visual spatial information from the parietal association cortex and is most needed for performance of the ODR task. (*D*) Etazolate effect on a dlPFC delay cell from a young monkey (9 y). Etazolate (5 nA) significantly reduced delay-related firing compared with control conditions ($P < 0.05$, one-way ANOVA). Only firing for the neuron's preferred direction is shown. (*E*) Etazolate effect on a dlPFC delay cell from an aged monkey (21 y). Etazolate (5 nA) did not significantly alter delay-related firing compared with control conditions, whereas the higher dose (25 nA) significantly reduced firing ($P < 0.05$, one-way ANOVA). Only firing for the neuron's preferred direction is shown.

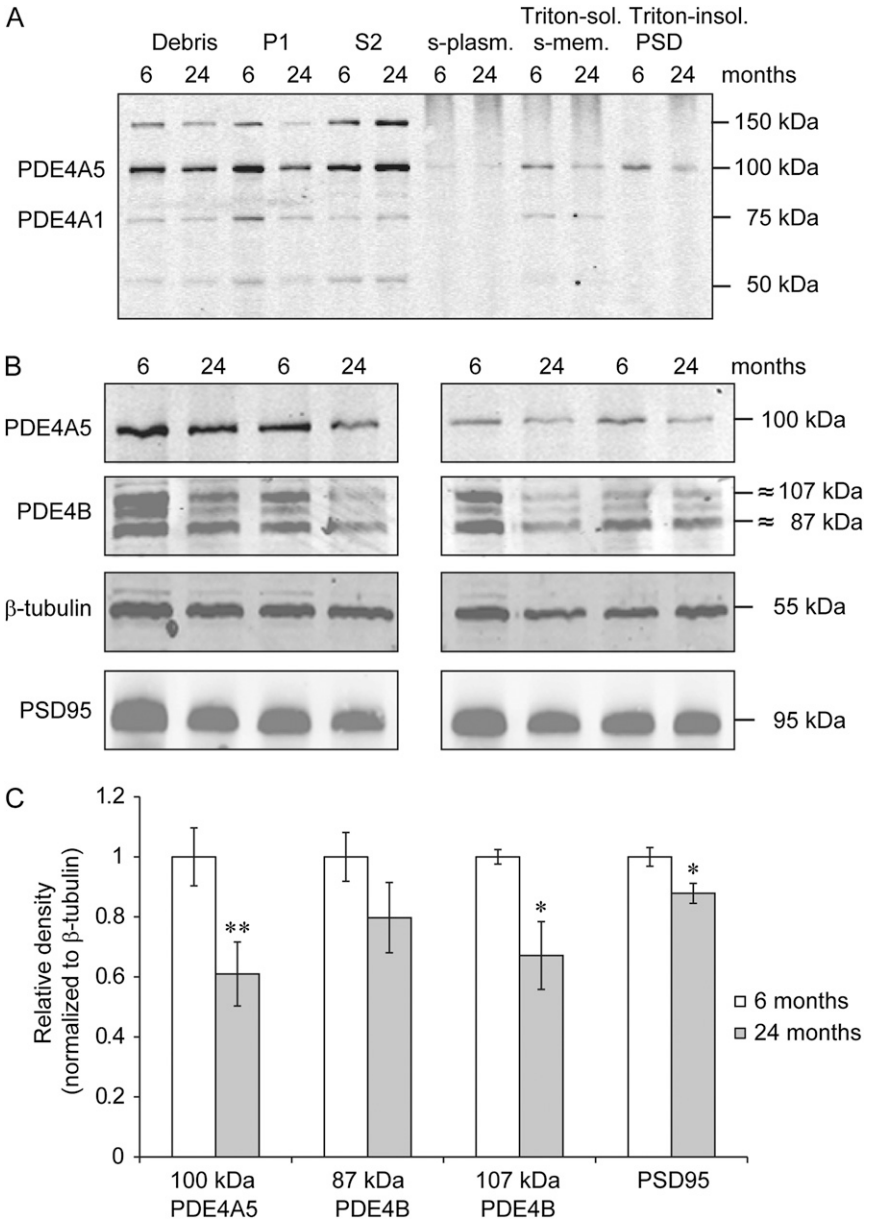

Fig. S6. Distribution of PDE4s through the mouse postsynaptic density (PSD) preparation. (*A*) Immunoblot showing the segregation of PDE4A isoforms throughout the stages of the PSD preparation process. The blot used one sample from a 6-mo-old and one sample from a 24-mo-old mouse. Only PDE4A5 is detectable in the Triton-insoluble PSD fraction. (*B*) Immunoblots showing the data quantified in Fig. 5*C*. Blots depict Triton-insoluble PSD fraction staining for PDE4A5 (Abcam; ab14607), PDE4B (1), β-tubulin (Sigma), and PSD95 (EMD Millipore). Each band represents tissue pooled from two animals of the same age: $n = 4$ pools per age group. (*C*) PDE4A, PDE4B, and PSD95 bands were quantified and normalized to β-tubulin to control for protein loading. PDE4A and PDE4B bands were further normalized with regard to PSD95 intensity to account for observed PSD loss. $^{**}P < 0.05$, remained significant ($P < 0.05$) when also normalized by PSD95 levels. $^{*}P < 0.05$, significance was lost after correction for PSD95 intensity. Error bars represent SEM.

1. Huston E, et al. (1997) Molecular cloning and transient expression in COS7 cells of a novel human PDE4B cAMP-specific phosphodiesterase, HSPDE4B3. *Biochem J* 328(Pt 2):549–558.

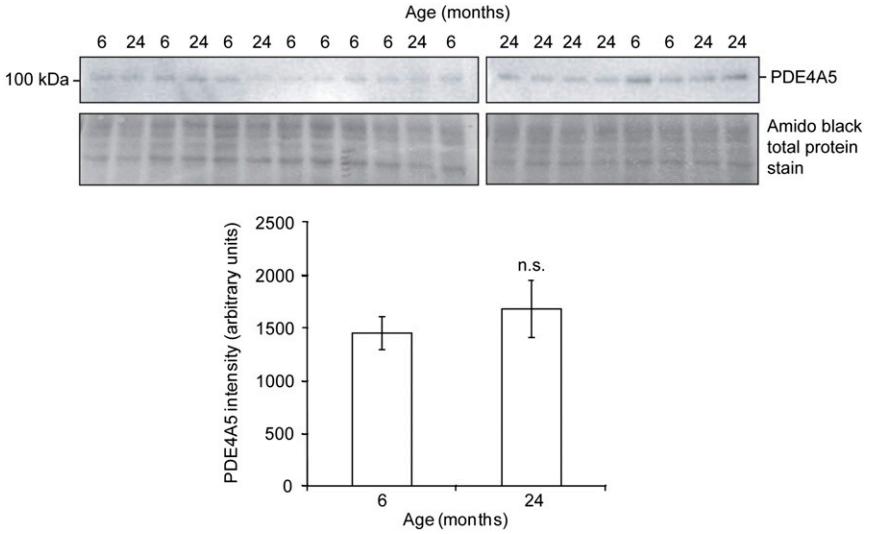

Fig. S7. PDE4A5 in total lysate from mouse PFC. Immunoblot was labeled for PDE4A (Abcam; ab14607) in 6-mo-old vs. 24-mo-old total tissue lysate from a punch of flash-frozen PFC. Note that the signal-to-noise ratio is low, reflecting the difficulty to discern PDE4A5 in total lysate from mouse brain. PDE4A5 band intensity was normalized by Amido black total protein stain (Sigma), and the quantification is shown in the graph. No significant effect of age on PDE4A5 expression was detected.

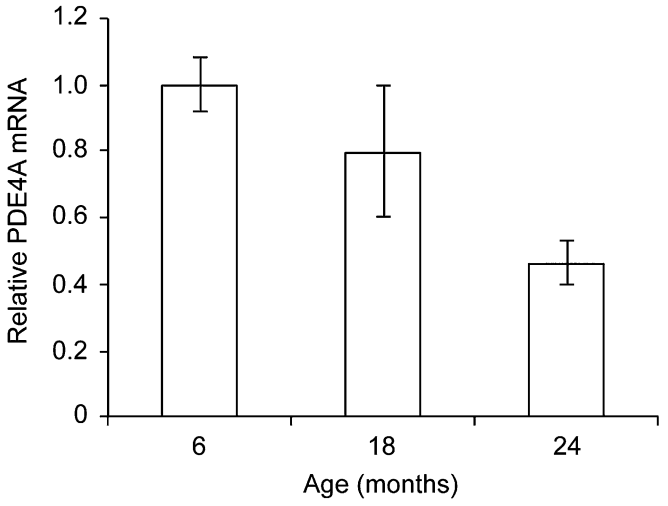

Fig. S8. qPCR using a pan-PDE4A probe shows a significant decrease in PDE4A mRNA with age in flash-frozen mouse PFC. Monotonic decrease in expression was found to be significant by one-way ANOVA; $P < 0.02$ [$F(2,18) = 5.185$]. Error bars represent SEM. Samples were normalized using probes for the reference genes TBP and RSP, which were found to be stable with increasing age. Forward pan-PDE4A probe, ACCACAACAGCCTGCACGCA; reverse pan-PDE4A probe, TGCCAGCTCCGAATTGGTGTTG.

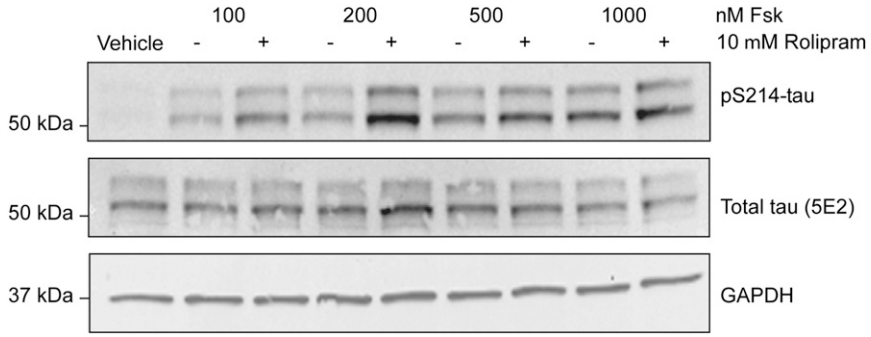

Fig. S9. Effect of PDE4 inhibition on phosphorylation of tau at S214. Sample immunoblot (one representative experiment of seven) depicts data summarized in Fig. 5*D*. Mouse primary cortical neurons (7–11 d in vitro) were preincubated with 10 μM rolipram or vehicle for 10 min, before being subjected to varying concentrations of forskolin (100–1,000 nM). Following treatment, cells were lysed in 1% SDS with protease and phosphatase inhibitors (Complete Mini, Roche; and PhosStop, Roche) and heated to 70 °C to prevent further phosphatase activity. Samples were quantified by bicinchoninic acid assay and analyzed by immunoblotting. Blots were labeled for pS214-tau (Abcam; 4846), total tau (EMD Millipore; clone 5E2) and GAPDH (Advanced Immunochemical; mAb 6C5). Bands were quantified using Image J, and total tau signals were normalized by GAPDH. p-Tau signals were then normalized to total tau signals.